

HARVARD COLLEGE OBSERVATORY

60 GARDEN STREET  
CAMBRIDGE, MASSACHUSETTS 02138

1N-92-CR  
84778  
p-16

STATUS REPORT

October 1, 1991

NASA Grant NAGW-1687

Laboratory Studies in Ultraviolet  
Solar Physics

Principal Investigator: W. H. Parkinson

Co-Investigators:

J. L. Kohl

L. D. Gardner

J. C. Raymond

P. L. Smith

The Harvard College Observatory  
is a member of the  
Harvard-Smithsonian Center for Astrophysics

(NASA-CR-190240) LABORATORY STUDIES IN  
ULTRAVIOLET SOLAR PHYSICS Status Report,  
period ending 30 Sep. 1991 (Harvard Coll.  
Observatory) 16 p

N92-26029

Unc1as  
G3/92 0084778

## 1. INTRODUCTION

This is a Status Report as of 9/30/91 for the grant *Laboratory Studies in Ultraviolet Solar Physics* NASA, NAGW-1687. The research activity of the Grant comprised the measurement of basic atomic processes and parameters which relate directly to the interpretation of solar ultraviolet observations and to the development of comprehensive models of the component structures of the solar atmosphere. The research was specifically directed towards providing the relevant atomic data needed to perform and to improve solar diagnostic techniques which probe active and quiet portions of the solar chromosphere, the transition zone, the inner corona, and the solar wind acceleration regions of the extended corona. The accuracy with which the physical conditions in these structures can be determined depends directly on the accuracy and completeness of the atomic and molecular data.

These laboratory data are used to support the analysis programs of past and current solar observations (*e.g.*, the Orbiting Solar Observatories, the Solar Maximum Mission, the Skylab Apollo Telescope Mount, and the Naval Research Laboratory's rocket-borne High Resolution Telescope and Spectrograph). In addition, we attempted to anticipate the needs of future space-borne solar studies such as from the joint ESA/NASA Solar and Heliospheric Observatory (SOHO) spacecraft.

Our laboratory activities stressed two categories of study: (1) the measurement of absolute rate coefficients for dielectronic recombination and electron impact excitation and (2) the measurement of atomic transition probabilities for solar density diagnostics.

In the following sections we will provide a brief summary of the research activity.

Our laboratory studies in solar physics are continuing with support from NASA Grant NAGW-1687 for the period 10/1/91 - 9/30/92.

## 2. THE MEASUREMENT OF ABSOLUTE RATE COEFFICIENTS FOR DIELECTRONIC RECOMBINATION AND ELECTRON IMPACT EXCITATION

### 2.1 Introduction

This section describes accomplishments in the area of dielectronic recombination (DR) measurements and their application to ionization balance calculations for the solar transition region. Accomplishments can be grouped into three primary areas: (1) Experimental results for DR of  $C^{3+}$  in a known external electric field, (2) Results of a study of the effects of electric field enhanced DR on the ionization balance of carbon in the solar transition region, and (3) Progress toward measurements of the  $C^{3+}$  DR rate coefficient as a function of external field strength.

An initial experiment to measure the  $C^{3+}$  DR rate coefficient in a known external field was completed (Young 1990; Young *et al.* 1992). The DR process studied in this work involves the  $2s\ ^2S_{1/2} \rightarrow 2p\ ^2P_{3/2}$  transition in a  $C^{3+}$  ionic core and capture of an electron into a high Rydberg state. The experimental approach is based on the detection of the stabilizing photon (a satellite of the  $C^{3+}$  (2s-2p) transition at 155 nm) in delayed coincidence with the  $C^{2+}$  recombined ion. The rate coefficient for this process is believed to be sensitive to external electric fields in the ion rest frame. The inclined-beams geometry of the present experiment permits the application of known external electric fields whose strengths can be adjusted. The measured rate coefficient,  $(3.6 \pm 1.5) \times 10^{-10} \text{ cm}^3 \text{ s}^{-1}$  (at the 68 percent confidence level), was determined for an external field strength of  $12 \text{ V cm}^{-1}$ , an electron beam with an energy spread of 1.8 eV (FWHM) in the ion

rest frame and an electric field strength in the final ion charge state analyzer of  $4.9 \text{ kV cm}^{-1}$ . The measured value is 7.2 times larger than the zero field calculations of McLaughlin and Hahn (1983), and a factor of 5.1 over the corresponding calculations of Griffin *et al.* (1985). LaGattuta (1985) and Griffin *et al.* (1985) predict enhancements at  $12 \text{ V cm}^{-1}$  of 2.6 and 2.9 respectively. Field enhancement is required in the theory to predict a rate coefficient that approaches our experimental value. The factor of 2.5 - 2.8 difference between the theoretical and measured enhancements, falls within the experimental uncertainty at the 90 percent confidence level. However, our result for a known field together with the results of Dittner (1988) for an unknown external electric field suggest that the enhanced rates may be larger than predicted.

We investigated the implications of field enhancement of DR on the ionization balance of carbon (Reisenfeld *et al.* 1992, Reisenfeld 1992). It was found that plasma microfields have a strong influence on the density dependence of dielectronic recombination, particularly for Li-like ions. Consequently, spectroscopic observations of environments where high-temperature DR is important may need reinterpretation. As a first step we have computed the carbon ionization balance in the solar transition region using field enhanced rates, showing the need for increased emission measures to match C IV emission-line intensity observations. The DR rate is also highly sensitive to macroscopic electric and magnetic fields. This may have a profound effect on emissivities, particularly in active regions, and may ultimately lead to a diagnostic technique for field strengths in the solar transition region and corona.

Following our  $\text{C}^{3+}$  DR measurements at an external electric field strength of  $12 \text{ V/cm}$ , we initiated a measurement of the DR rate coefficient as a function of the external electric field strength. This work, which is in progress, required several improvements to the apparatus and techniques. Progress on this measurement will be described in section 2.4.

## 2.2 Measurement of $\text{C}^{3+}$ Dielectronic Recombination in a $12 \text{ V cm}^{-1}$ External Field

In this section, we describe our measurement of  $\text{C}^{3+}$  DR in a  $12 \text{ V cm}^{-1}$  external field. We begin with a brief description of the apparatus followed by a summary of the experimental results.

The basic experimental arrangement used for the present measurements has been described by Gardner *et al.* (1986) and Lafyatis, Kohl and Gardner (1987). Charge-to-mass-selected, accelerated, and focused ions from an oscillatory discharge source (Mavrogenes *et al.* 1965) are deflected  $90^\circ$  in a beam switching magnet to remove lower charge states produced by charge exchange collisions with the background gas. After leaving the switching magnet, the beam is electrostatically steered and then refocused into the interaction chamber with a magnetic quadrupole triplet lens. The beam size and position in the chamber are independently controlled.

Figure 1 is a diagram of the arrangement in the interaction chamber. The interaction chamber itself is designed for ultrahigh vacuum and provides about  $1 \times 10^{-10}$  Torr during experiment operation. The ion beam enters the chamber and passes through an electrostatic charge state analyzer which rids the beam of charge states other than the ionic species of interest. Near the center of the interaction chamber the ion beam crosses an electron beam inclined at an angle of  $45^\circ$ .

The electron gun, which produces the electron beam, has a dispenser cathode, a control grid and anode, and is focused with a three-element electrostatic lens. An axial magnetic field provided by two magnetic field coils is used to confine the electron beam. Electron currents in excess of  $40 \mu\text{A}$  are obtained with a 20 Gauss confining field. The beam can be pulsed at frequencies up to 10 MHz. The axial magnetic field results in

a motional electric field in the ion rest frame. The electric field can be set at the value of interest by selecting the corresponding coil current.

The ion and electron beams are probed with Faraday cups which have apertures of  $130\ \mu\text{m}$  diameters. They are scanned in two dimensions through each beam. Probes are done under software control with automatic recording of the ion or electron beam current as a function of probe position. Form factors and integrated ion and electron beam currents are then calculated using computer programs operating on a VAX computer.

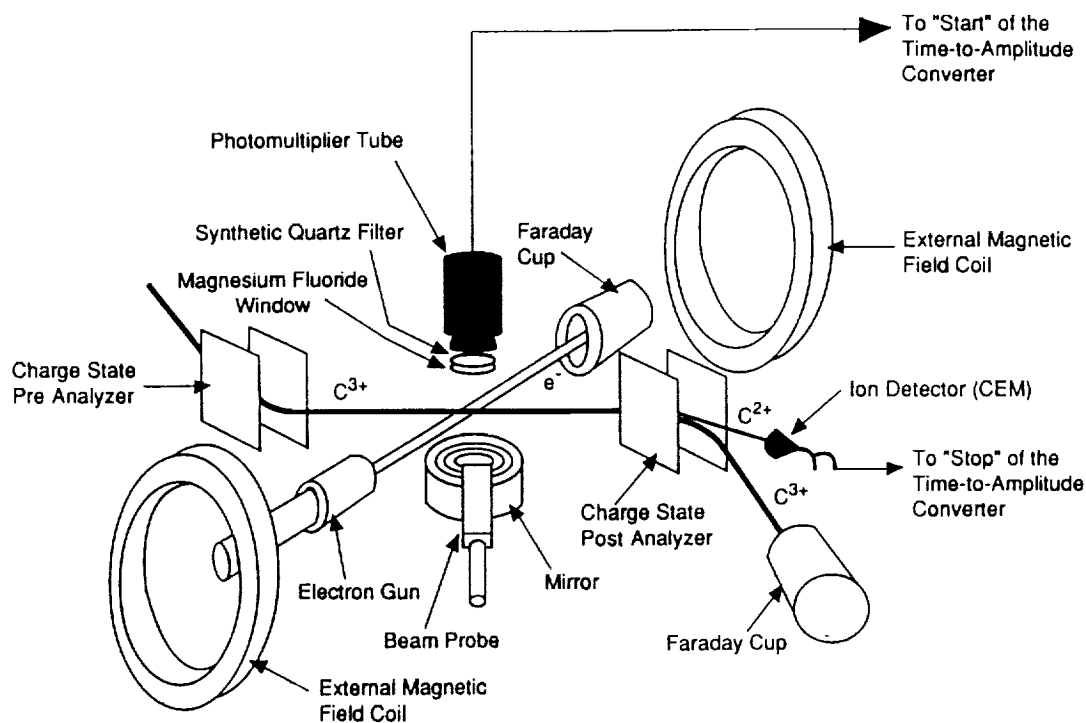


Figure 1. Experimental arrangement inside the electron-ion interaction chamber.

The charge state post analyzer is used to separate recombined ions from the primary ions in the beam. For DR, recombined ions are detected by a particle detector (*i.e.*, a channel electron multiplier, CEM).

The region of intersection of the two beams is continually monitored by a photon collection and detection system. To make an absolute measurement of DR, it is necessary to measure, absolutely, a known fraction of the photons produced. The photon collection and detection system used for this work consists of a mirror with a  $\text{MgF}_2$  overcoated aluminum coating which collects photons from the beams intersection region and directs them onto a detector — a solar blind photomultiplier tube which is operated in a pulse counting mode. The mirror system, which was developed for the present measurement, collects 25 percent of the photons emitted from the ion/electron beams' intersection region. This is an 18-fold improvement over the arrangement used for our previous measurements. The wavelength bandpass of the system is determined by the long wavelength cut-off of the photomultiplier tube and the short wavelength transmission limit of a filter.

The DR rate coefficient can be expressed as a function of experimentally determined quantities as follows:

$$\begin{aligned} \langle v\sigma_{DR} \rangle_E &= \int \sigma_{DR}(E)v_r(E)P(E)dE \\ &= \frac{S_{DR}}{\xi \int N_I(x,y,z)n_e(x,y,z)I(x,y,z)\eta(x,y,z,\tau)dx dy dz} \end{aligned} \quad (\text{Eq. 1})$$

The rate coefficient is defined as an integral over the electron's energy, involving  $\sigma_{DR}(E)$ , the DR cross section as a function of energy,  $v_r(E)$ , the relative velocity between the ions and electrons, and  $P(E)$ , the probability an electron will have an energy between  $E$  and  $E+dE$ . On the R.H.S.,  $S_{DR}$  is the signal due to DR,  $\xi$  is the fraction of the beam in the ground state of  $C^{3+}$ ,  $N_I(x,y,z)$  is the ion density,  $n_e(x,y,z)$  is the electron density,  $I(x,y,z)$  is the detection efficiency for recombined ions, and  $\eta(x,y,z,\tau)$  is the total photon detection efficiency.  $\eta(x,y,z,\tau)$  can be written as follows:

$$\eta(x,y,z,\tau) = \epsilon(x,y,z,\tau)Y_{\Omega}(x,y,z),$$

where  $\epsilon(x,y,z,\tau)$  is the detection efficiency for the photons ( $\tau$  is the lifetime of the radiative process), and  $Y_{\Omega}(x,y,z)$  is the angular anisotropy factor for the emitted photons. The integral in the denominator of Eq. 1 is called the overlap-efficiency (OE) integral. An experimental determination of the rate coefficient consists of evaluating each of the elements of the R.H.S. of this equation. For a comparison to theoretical predictions of the cross sections,  $v_r(E)$ ,  $P(E)$ , and the electric fields in the experiment must be specified as well.

The electron impact excitation (EIE) rate coefficient for the  $1s^22s^2S$  to  $1s^22p^2P^o$  transition ( $2s - 2p$ ) in  $C^{3+}$  was measured before and after the DR experiments. The experimental arrangement for EIE is the same as that for DR. Near-threshold EIE data taken prior to and after the DR experiment provided the absolute scale for the ion rest frame energy of the electrons, the energy distribution of the electrons and the photon detection efficiency.

The experimental approach for EIE was similar to that described by Layfatis *et al.* (1987). Each measurement involved switching the electron cathode potential between two different values. One value was usually set at a reference voltage above threshold (a cathode potential of 15.75 V). The repeated measurement of the cross section at this point provided a consistency check on the EIE experiment. The other value of the cathode potential was adjusted to provide EIE data points across the threshold for the EIE process.

The absolute photon detection efficiency for the DR experiment is determined by normalizing the measured EIE rate coefficient to theory. The EIE rate coefficient data, normalized to the theory, are provided in Fig. 2 (error bars represent the statistical uncertainty at the 90 percent confidence level). The lowest energy point overlapped with zero, largely eliminating the possibility of a significant spurious signal associated with beam-modulated background.

Normalization to theory involves the convolution of the theoretical cross section with the experimental energy distribution. The analytical expression for the cross section versus energy is taken from the two state close-coupling work of Gau and Henry (1977). Their results are found to be in good agreement with other calculations (Mann 1980,

Robb 1980). The effect of higher lying states on this cross section (near threshold) was found to be negligible (Bhadra & Henry 1982). The free parameters were varied to determine the best fit and to estimate the range of values that are consistent with the data (i.e., correspond to a value of  $\chi^2$  less than 1). The FWHM of the electron beam energy distribution in the ion rest frame was found to be  $1.80 \pm 0.47$  eV, and the offset potential was similarly found to be  $1.71 \pm 0.26$  V.

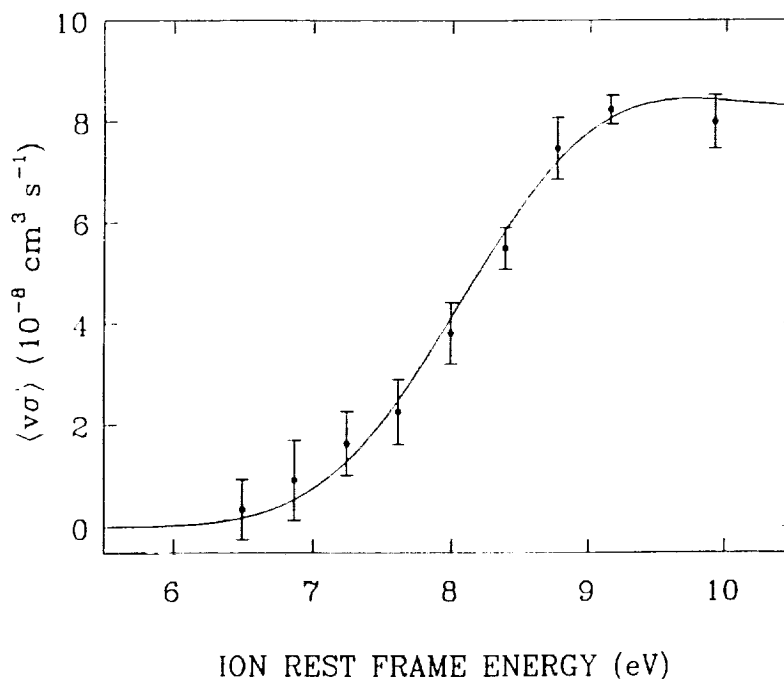


Fig. 2. The EIE rate coefficient near threshold for the  $1s^2 2s^2 S$  to  $1s^2 2p^2 P^o$  transition in  $C^{3+}$ . The solid curve is the best fit of the experimental data to theory. The error bars on the data are statistical uncertainty at the 90 percent confidence level.

The DR event rate ( $S_{DR}$  in Eq. 1) is determined by detecting stabilizing photons in delayed coincidence with recombined  $C^{2+}$  ions. The signal is obtained by subtracting a coincidence trace with the electron beam off from a coincidence trace with the electron beam energy centered on the expected DR peak. The electron beam energy was switched every 10 seconds over each thousand second run. The difference trace after being corrected for dead time should be flat outside the coincidence window and exhibit a peak inside the coincidence window. The coincidence window is the range of delay times between the detection of stabilizing photons and the detection of recombined ions from individual DR events. The location of the DR window on the coincidence trace was determined by detecting photons and  $C^{2+}$  ions from  $H_2 + C^{3+}$  charge transfer into excited  $C^{2+}$  states (see Gardner *et al.* 1986). The DR signal is extracted by fitting the background outside the window with a least-squares fit and subtracting this from the difference spectrum. The number of counts remaining in the coincidence window divided by the time spent with the electron energy on-resonance is the signal. The current in the magnetic coils, which were used to apply fields in the interaction region, varied by less than one percent for all measurements. The backgrounds and currents were monitored for each run. These monitor data were used to evaluate each run and to compute average background rates.

The DR measurement is the result of nine runs: four with the cathode potential at 14.25 V and five at 14.50 V. Because the energy distribution was about 2.4 eV wide (FWHM) in the laboratory frame, the difference in energy did not make a significant change in the rate coefficient. The value for the final rate coefficient was computed using

an average of the nine measured rate coefficients weighted so that the most reliable data have the largest weight (Leo 1987).

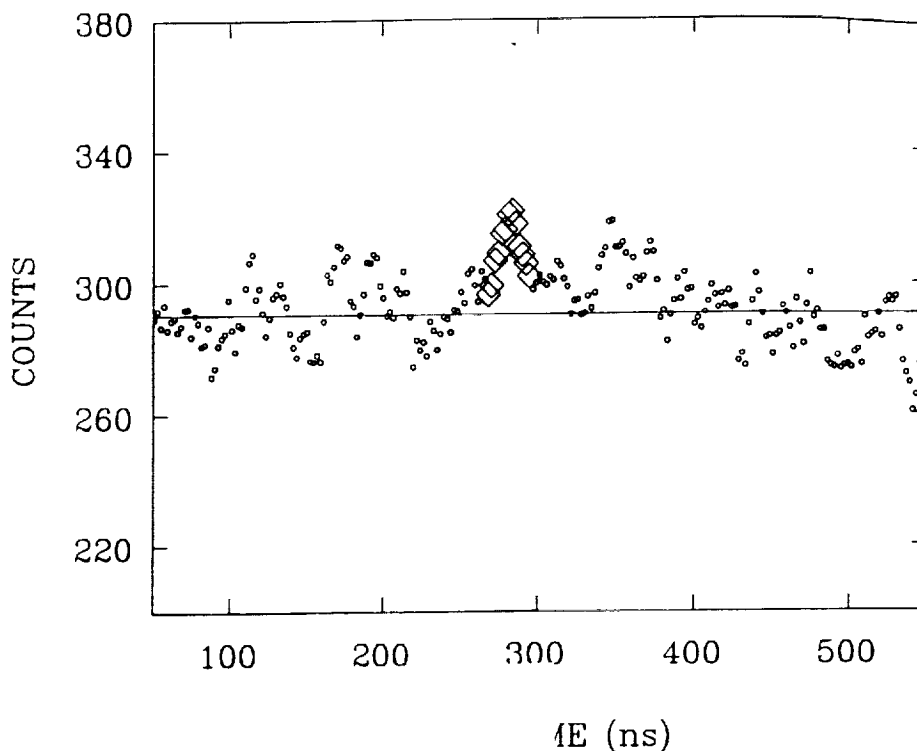


Fig. 3. The sum of all the DR coincidence data, with a running sum over 11 ns (to smooth some of the statistical fluctuations in the coincidence data). Data within the coincidence window are indicated by diamonds. A linear fit to the background data is also shown.

The sum of all the difference traces is shown in Fig. 3. These data are presented as a running sum of the DR coincidence data over an 11 ns interval, showing the signal inside the coincidence window (indicated by diamonds) more clearly. Although the final result was derived from rate coefficients obtained for each run separately, this sum exhibits several important features of the coincidence data. Outside of the coincidence window, the trace is flat. This is consistent with the idea that this background is due to accidental coincidences. This background was determined by fitting the data outside the coincidence window with a linear least-squares fit. The resulting slope of this line produced a drop in the average level of the background of 2.3 counts (out of an average of 290) from one end of the coincidence trace to the other. The statistical uncertainty for a single point in these data is about  $\pm 20$  counts (the uncertainty resulting from Poisson statistics, with the total number of counts for each channel given by the sum of the data in the "on" and "off" resonance coincidence trace). The statistical uncertainty in the average value of the background is  $\pm 1.3$  counts. Thus the slope is not a statistically significant feature of the background.

Another satisfying feature of the data is that the  $\chi^2$  per degree of freedom for the deviations of the background data from the line generated by the least-squares fit is 1.04. Since there is a 33 percent chance of randomly observing a larger value of  $\chi^2$ , this indicates a reasonable statistical distribution of points around the line. A check for large scale structure in the background is to add a quadratic term to the fit. Adding this term reduces the signal computed from the data by 32 percent. This change is on the order of the statistical uncertainty of the signal ( $\pm 30$  percent at the 68 percent confidence level), and indicates that this does not produce a statistically significant change in the DR

measurement. Hence, the background is assumed to be flat, consistent with an expectation of a background due only to accidental coincidences.

The final result measured for the DR rate coefficient at a peak ion rest frame energy of  $8.01 \pm 0.20$  eV is  $(3.6 \pm 1.5) \times 10^{-10}$  cm<sup>3</sup>s<sup>-1</sup> and the energy averaged cross section is  $(2.1 \pm 0.9) \times 10^{-18}$  cm<sup>2</sup> (both uncertainties are quoted at the 68 percent confidence level). The sources of the uncertainties quoted above are displayed in Table I. This measurement is dominated by statistical uncertainties ( $\pm 30$  percent, quoted here at the 68 percent confidence level). The absolute scale for the DR measurement is partially determined by normalizing the EIE energy-averaged cross section to theory. The scale factor  $\epsilon_\gamma$ , deduced by the fitting procedure discussed previously, is  $(6.9 \pm 1.0) \times 10^{-3}$ . The uncertainty in the normalization procedure is the sum, in quadrature, of the (statistical) uncertainty in the scale factor and the OE integral variability (see Eq. 1). The total is  $\pm 14$  percent. The uncertainty in the uniformity of the PMT response introduces a  $\pm 19$  percent uncertainty into this normalization procedure.

Table I: Sources of uncertainty for the DR measurement.

Sources of uncertainty	Uncertainty
Overlap integral normalization	14%
Uncertainty in PMT uniformity	19%
Variation in the overlap integrals during a run	12%
Variation in CEM efficiency	15%
Absolute ion detection efficiency	4%
Statistics ( $1\sigma$ )	30%
Sum in quadrature ( $1\sigma$ )	43%

The OE integral variability enters again through the uncertainty of the OE integrals used to reduce the DR data itself. This contributes an additional  $\pm 11$  percent to the quadrature sum of uncertainties. The variability in the CEM efficiency is also sizable ( $\pm 15$  percent). The uncertainty in the absolute ion detection efficiency is fairly small ( $\pm 4$  percent). The overall absolute uncertainty at the 68 percent confidence level is  $\pm 43$  percent.

Photon anisotropy factors, as they pertain to this inclined beams geometry, have been discussed elsewhere (Lafyatis *et al.* 1987; Young 1990). The large solid angle of photons collected from the interaction volume makes this experiment less sensitive to anisotropies in the emitted radiation than it would be with a more typical solid angle size used. The outer bounds for the size of these effects is  $+10$  to  $-21$  percent. If fine-structure depolarization effects are considered, these limits are tightened to  $+3$  to  $-6$  percent. The effects of the captured electron on the anisotropy expected from DR has not yet been treated theoretically for systems similar to C<sup>3+</sup>. These effects may alter the limits due to fine structure depolarization, but do not affect the outer limits quoted. The size of the experimental error bars prohibits detailed investigation of the effects of anisotropy at the present time.

The measured rate coefficient can now be compared with theory. The energy distribution derived from the excitation data, the electric fields, and the cutoff principal quantum number,  $n$ , of the captured electron due to field-ionization of the recombined



ions in the post-analyzer (calculated, using the usual hydrogenic formula [Brouillard 1983] to be  $n_{max}=43$ ) serve to unambiguously determine the conditions under which the DR rate coefficient was measured. Table II lists the DR rate coefficient measured in this work and predicted DR rate coefficients for no external electric field and for an external field strength of  $12 \text{ V cm}^{-1}$ .

**Table II: Comparison of DR rate coefficient measurement to theoretical prediction (using the experimental energy distribution presented in Fig. 2). F denotes the external field strength. Experimental uncertainties are absolute, and at the 90 percent confidence level.**

Source	Rate coefficient ( $\times 10^{-10} \text{ cm}^3 \text{ s}^{-1}$ )	
	F=0 V/cm	F=12 V/cm
Present work		$3.6 \pm 2.5$
LaGattuta (1985), McLaughlin and Hahn (1983)	0.5	1.3
Griffin (1985,1989)	0.7	2.0

There are several points to note concerning these calculations. The first is that the present experimental result differs from the theoretical zero field rate coefficients (at the 90 percent confidence level). The field effect is required to produce agreement with theory. The second is that the measured value of the rate coefficient is a factor of 2.8 larger than that predicted by combining the enhancement calculations of LaGattuta (1985) with the zero field cross section of McLaughlin and Hahn (1983) and a factor of 1.8 larger than that predicted by Griffin (1989) and Griffin *et al.* (1985), although the experimental uncertainties may account for the differences. The work of Dittner (1988) also indicated a rate coefficient that is larger (by a factor of 1.5) than rate coefficients predicted by Griffin *et al.* (1985). The recent work of Anderson *et al.* (1990) (for fields estimated to be 2 to  $3 \text{ V cm}^{-1}$ ) is at most a factor of 1.12 larger than theory. It should be noted that the fields were not precisely known in either of these latter experiments.

The rate coefficients calculated by Griffin are generally larger than those of LaGattuta (1985) and McLaughlin and Hahn (1983). One of the principal differences between the two calculations is that the work of Griffin includes fine structure interactions (it is an intermediate coupling calculation). Also, the size of the field enhancement appears to be smaller when intermediate coupling calculations are performed.

A final point is that neither of these calculations takes into account the field rotation effects on the measured recombination rate coefficient or the possibility of overlapping-interacting resonances. The rotation effects arise because the rest-frame electric fields in the collision volume and in the post-analyzer are at  $90^\circ$  to one another in the present experiment. The recombined ions therefore experience an electric field that is changing in orientations and magnitude, a situation which is known to affect the relative populations of the Stark states of the captured electron. This in turn, can affect the probability that the recombined ion is field-ionized in the post-analyzer. This has been studied in some detail for the case of  $\text{Mg}^+$  and resulted in a maximum reduction of 15 percent in the size of the predicted rate coefficient (LaGattuta, Nasser, and Hahn 1985). A similar effect may be present in  $\text{C}^{3+}$ . Analytical treatments using quantum defect theory indicate there may be a reduction in the size of the field enhancement at large values of the captured electron's principal quantum number due to overlapping-interacting resonances (Harmin 1987). This, too, would result in a

small decrease in the size of the predicted rate coefficient. Both effects tend to push the experimentally determined rates out of agreement with theory, but the effects are expected to be small and should not result in a dramatic change to the conclusions drawn from the experiment.

### 2.3 Electric Field Enhanced Dielectronic Recombination in the Solar Transition Region

We investigated the implications of DR field enhancement on the ionization balance of carbon in the solar transition region. The electric fields that were considered in the study are ion microfields Griem (1964). The code of Raymond (1988) was used to investigate the ionization balance for three cases: a theoretical value for DR with no enhancement, a theoretical value with enhancement due to the ion microfields, and an enhancement of DR in  $C^{3+}$  that reflects the increase in our experimental values over theory. The results are illustrated in Figure 4. The theoretical enhanced DR rate for  $C^{3+}$  affects the ionization balance by suppressing the  $C^{3+}$  charge fraction by as much as a factor of two over the temperature range where it experiences significant ionization.

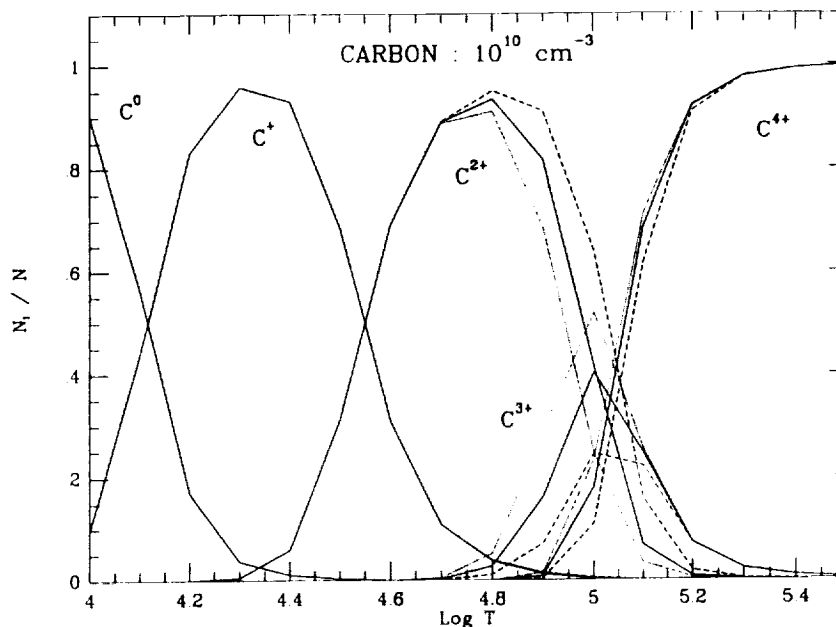


**Figure 4.** The carbon ion charge fraction as a function of solar transition region temperature at a plasma density of  $1 \times 10^{10} \text{ cm}^{-3}$ . The effects of zero-field DR (dot-dash trace) and field enhanced DR (solid and dashed traces) are compared. All DR rates are theoretically calculated, except the dashed trace uses theoretical rates rescaled to reflect the factor of 2.6 between our experimentally determined DR cross section and the theoretical cross section of LaGattuta (1985). The source of the electric field modeled here is the plasma microfield arising from the hydrogen ions. At  $1 \times 10^{10} \text{ ions/cm}^3$  this field has a strength of about 6 V/cm, comparable to the electric fields at which our experimental data are taken. The enhancement of the  $C^{3+}$  DR rate affects the ionization balance in two major ways. Over the temperature range where  $C^{3+}$  is ionized, its abundance is suppressed by as much as a factor of 2 in the pure theoretical case and as much as a factor of 4 in a rescaled case. By contrast, the  $C^{2+}$  charge fraction undergoes a reciprocal enhancement in abundance, leading to an upward shift in the temperature at which the charge fraction peaks. The shift amounts to an increase of  $6 \times 10^3 \text{ K}$  in the pure theoretical case and  $1 \times 10^4 \text{ K}$  in the rescaled case.

There is also an increase on the  $C^{2+}$  charge fraction and an upward shift by 6000 K in the temperature of peak abundance. The enhancement is even more pronounced if the larger experimental rates are considered. There may well be fields in addition to the ion microfields such as DC fields associated with coronal heating, fields generated by plasma turbulence, and Lorentz fields (Foukal & Hinata 1991). The present result should be taken as only a rough model of the transition region, as we neglect physical mechanisms such as steady state diffusion and time dependent motions, as well as the influences of a possible non-Maxwellian velocity distribution. These effects are summarized in a paper by Raymond (1988).

#### 2.4 Progress Toward Measurements of $C^{3+}$ DR as a Function of the External Field Strength

Following the measurement of DR at 12 V/cm, we initiated a measurement to determine the DR rate in  $C^{3+}$  for more than one field strength. In addition to determining the DR rate as a function of field strength, these measurements are expected to help determine if the field enhancement part of the theory is having difficulties or if there is a problem in predicting the basic rate.

Several improvements were made to the experiment which increased the sensitivity and decreased the backgrounds of the experiment. The present arrangement has a factor of three improvement in the sensitivity and a factor of more than three in reduced backgrounds. The spatial uniformity of the PMT was improved significantly; this nearly eliminated the previous  $\pm 19\%$  uncertainty. Magnetic field measurements that determined the ion rest frame electric field strength for four settings (corresponding to 0.7, 2.8, 12, and 21 V/cm) were also completed. The techniques for calibrating the section of the experiment used for detecting  $C^{2+}$  ions was improved. We also evaluated and improved our method for determining the distribution of ions and electrons in the beams.

The new DR measurements are underway. The first step, which has now been completed, was to measure the  $C^{3+}(2s-2p)$  EIE rate coefficient in order to determine the photon detection efficiency, electron energy spread and absolute electron energy scale for the improved experimental conditions. The results of that measurement are provided in Figure 5. The analysis approach for the new EIE data was similar to that described in section 2.2.

The measurement of DR versus field strength is the Ph.D. thesis research of Daniel W. Savin. The project consists of repeating the measurement for 12 V  $cm^{-1}$ , but with improved uncertainty limits and then determining the rate coefficient for at least one other field value. The plan is to make the second measurement at about 1 V  $cm^{-1}$ .

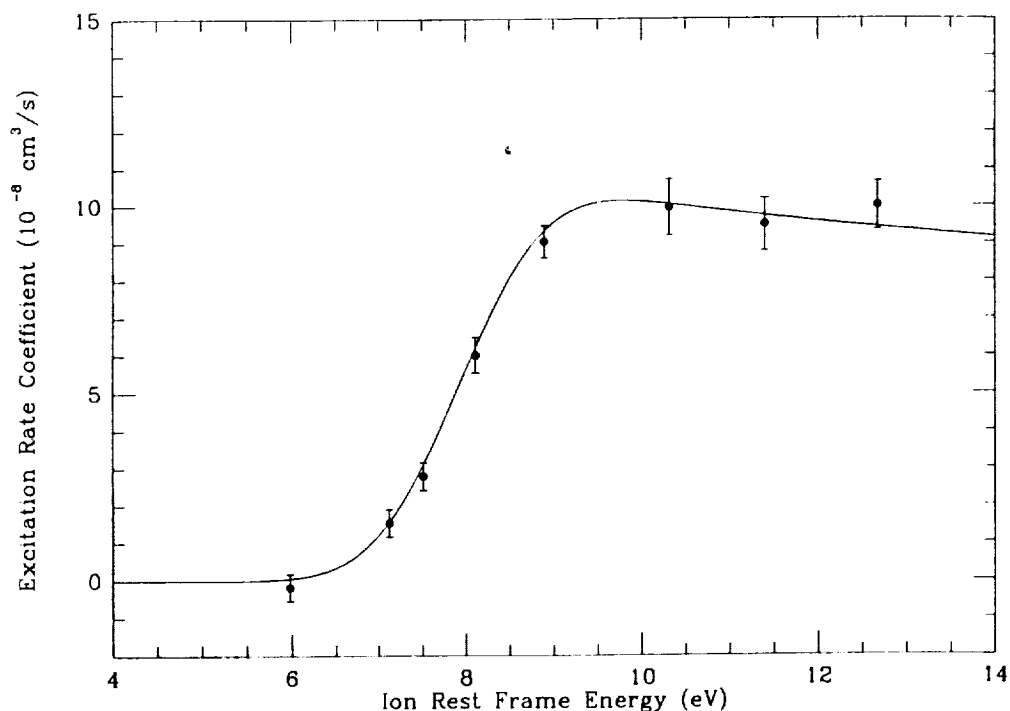


**Figure 5.** The EIE rate coefficient measurement (points) and normalization to theory (solid line). This information determines the absolute electron energy scale, the electron energy spread and the photon detection efficiency for the present DR measurements.

### 3. MEASUREMENTS OF ATOMIC TRANSITION PROBABILITIES FOR SOLAR DENSITY DIAGNOSTICS

#### 3.1 Introduction

One of the major goals of our research program is the measurement of transition probabilities ( $A$ -values) for spin-changing (intersystem) lines of light atomic ions. In diffuse plasma, like the solar chromosphere, and the corona, the rates for radiative decay (transition probabilities), of metastable atomic levels can be the same order of magnitude as the rates for excitation and deexcitation by electron collisions. Intensity ratios involving lines from metastable levels are sensitive to electron densities and temperatures and are often the basis of the best diagnostic techniques. None of the intersystem-line  $A$ -values that are used in solar electron density and temperature determinations had been measured until we began our laboratory program with this goal. Calculated  $A$ -values are often not in agreement, and our results show that the uncertainties for some calculated values may have been underestimated.

#### 3.2 General Experimental Method; the Ion Trap

We measure the radiative lifetimes of the upper levels of the transitions of interest, and make use of the relationship between the radiative transition probabilities for decays from an excited level,  $j$ , and its radiative lifetime,  $\tau$ ,  $\sum_i A_{ij} = \tau_j^{-1}$ . Because the lifetimes are of the order of  $10^{-4}$  to  $10^{-2}$  sec (about  $10^5$  times longer than those of 'allowed' atomic transitions), the upper levels are said to be metastable.

At room-temperature thermal velocities of  $\sim 5 \times 10^4$  cm sec<sup>-1</sup>, unconfined ions move about 5 to 500 cm before radiating. Thus, in order to measure the lifetimes, the ions must be confined in a collision-free manner. We do this with an 'ion trap', a 20-volt potential well created by a combination of radio-frequency (r.f.) and d.c. electric fields. The ions are created by electron bombardment of gases containing the atomic species of interest, or in a laser-produced plasma. Because the pressure in the apparatus is low ( $10^{-7}$  Torr), the environment is essentially collision-free and the ions decay radiatively.

The ion trap apparatus has undergone a series of modifications and upgrades during this recent grant period. Several in-house electronic and optical improvements, and also the purchase and incorporation of a multichannel scaler have modernized the apparatus. Much of the electronic work has centered on increasing the speed of high voltage circuits associated with trap operation, and also on developing signal detection circuitry compatible with the multichannel scaler. Many of the levels of ions of interest decay by emitting a VUV-photon, correspondingly, much of the system optics has been reworked with VUV detection the primary objective.

Tests of the upgraded ion trap system have been carried out by measuring radiative lifetimes of levels of ions that we had previously studied in detail as part of thesis research problems.

### 3.3 Intersystem-Line A-value Measurements

Some of the metastable levels of ions that we are studying (*e.g.*, Si II) or have studied (*e.g.*, O III) have several decay channels. Determination of the individual transition probabilities ( $A_{jk}$ ) from the measured lifetimes requires, either, a measurement of their branching ratio ( $BR_k^j$ ) by observing the individual line spectra from a suitable light source, or a measurement of time-resolved, laser-induced fluorescence from a selected excited level of the ion. We have used a Lambda-Physik excimer, laser-pumped, dye-laser with a barium borate crystal to frequency double the laser output. With this arrangement we have produced tunable, laser-line radiation at the wavelengths of the Si II intersystem multiplet  $3s^2 3p^2 P^o - 3p^2^4 P$  near  $\lambda$  234 nm.

We have also purchased a Si hollow-cathode which is constructed so that laser radiation can pass through the hollow-cathode and ring anode. We have tested this special hollow-cathode in standard operation and have recorded the two strongest of the three lines of the Si II resonance multiplet  $3s^2 3p^2 P^o - 3s 3p^2^2 D$  at 180.8, 181.6 and 181.7 nm.

#### *A-value for the C III 190.9 nm Intersystem Line*

The  $2s^2^1 S_0 - 2s 2p^3 P_1^o$  intersystem line of C III at 190.9 nm is one of the best and most often used lines in solar transition zone diagnostics (see Doschek 1985; Doschek *et al.* 1978; Raymond & Dupree 1978). Except for reports of our preliminary value (Smith *et al.* 1984a), no measured value for the transition probability of this line was available until our recent measurements. Theoretical A-values for the  $^1 S_0 - ^3 P_1^o$  transition in the BeI sequence are available from a number of detailed configuration interaction (CI) calculations (see Table III).

The lifetime of the  $^3 P_1^o$  level was obtained by direct observation of spontaneous emission from metastable  $C^{2+}$  ions stored in a radio frequency ion trap. We created the  $C^{2+}$  in our ion trap by electron bombardment of CO (and CH<sub>4</sub>). The trap was tuned to favor the storage of  $C^{2+}$ . By dumping and sampling with a mass spectrometer the ions that have been stored, we were able to tune the trap to improve

the storage of  $C^{2+}$ . The general storage technique and apparatus were similar to those used for our earlier measurements. However, two independent ion trap facilities were used in the C III measurements. The independent facilities allowed us to determine and reduce potential systematic errors, particularly those that might result from spectral and charge-to-mass resolutions available in these experiments. Our recently measured value is listed in Table III.

Table III: A-values (in  $\text{sec}^{-1}$ ) for the  $2s^2 \ ^1S_0$ - $2s2p \ ^3P_1^o$  Line of C III at 190.9 nm

experiment	75 ± 9%	our recent measurement
semi-empirical model potential	110 ± 15%	Laughlin <i>et al.</i> (1978)*
configuration interaction	96 ± 11%	Nussbaumer and Storey (1978)*
“ “ “	86 ± 10%	Glass and Hibbert (1978)
relativistic Hartree-Fock	75 ±	Cheng <i>et al.</i> (1979)
multi-configuration Hartree-Fock	110 ± 50%	Cowan <i>et al.</i> (1982)
multi-configuration Dirac-Fock	66 ± 15%	Bliman and Indelicato (1990)

\* the calculations marked disagree with our measured value by more than the combined limits of uncertainty.

#### Radiative Lifetime Measurement of Metastable Level in the Si Isoelectric Sequence

The  $^3P_{1,2} - ^5S_2^o$  intersystem lines of S III ( $\lambda 172.8939$  nm and  $\lambda 171.3117$  nm) were first discovered, not in a spectroscopy laboratory, but in emission from the Io torus with *I.U.E.* by Moos *et al.* (1983), who determined the wavelengths to within about 0.06 nm. These lines were thought to be potentially useful as solar density diagnostics if more precise wavelengths could be obtained and A-values and collision strengths determined. We found the lines on laboratory spectra, and refined the wavelengths to  $\pm 0.0005$  nm (Smith *et al.* 1984b). One of the lines, at  $1728.939 \text{ \AA}$ , was subsequently assigned to a previously unidentified solar spectral feature on the published line-test for the NRL solar spectrum from Skylab (Doschek *et al.* 1976); the other is masked by an Fe II blend (Cohen 1981).

Until now there were no measurements of radiative lifetimes of the  $3s3p^3 \ ^5S_2^o$  level for low Z-ions in the Si I sequence. The theoretical values differ by up to a factor of two (Ellis & Martinson 1984; Huang 1985; and Ellis 1989).

Since production of  $S^{++}$  and excitation by electron impact on a  $H_2S$  source vapor were expected to prove difficult, we decided to attempt a measurement of the radiative lifetime of the  $3s3p^3 \ (^5S_2^o)$  metastable level of  $P^+$ , the first ion in the Si sequence. A metastable  $P^+$  ion population was produced inside the cylindrical radio frequency ion trap by electron bombardment of  $PH_3$  vapour at pressure ranging from 5 to  $40 \times 10^{-8}$  Torr. Some of the light emitted by the decaying  $^5S_2^o$  population, was focused onto a 19 nm bandwidth interference filter, centered on 220 nm, in front of an EMR 541F photomultiplier tube used in the single-photon counting mode. The mean lifetimes was obtained from the decay rate parameter of a non-linear least-squares fit of a single exponential plus a constant background to the decay counts. Our measured result for the radiative lifetimes of the  $^5S_2^o$  level of  $P^+$  is  $167 \pm 12 \mu$ . Table IV summarizes the experimental and theoretical results. Ours is the first measured lifetime of the  $3s3p^3$

( $^5S_2^o$ ) level of a low charged-state ion in the Si I sequence. It will provide a test of the theoretical methods used to determine such  $A$ -values in low- $Z$  species of the Si I isoelectronic sequence, and it provided an excellent test of our ability to measure  $\mu$ s-scale lifetimes. A paper on this measurement has been submitted to and accepted by *Physical Review A*, 1992.

Table IV: Comparison of theoretical and experimental results for the radiative lifetime  $\tau_0$  of the  $3s3p^3$  ( $^5S_2^o$ ) metastable level of  $P^+$ .

Authors	$\tau_0$ ( $\mu$ s)	
Ellis & Martinson (1984)	519	Theory
Huang (1985)	272	Theory
Our recent measurements	$167 \pm 12$	Experiment

#### 4. REFERENCES

- Anderson, L. H., Bolko, J., and Kvistgaard, P. (1990), *Phys. Rev. A* **41**, 1293.  
 Bhadra, K., and Henry, R. J. W. (1982), *Phys. Rev. A* **26**, 1848.  
 Bliman, S. & Indelicato, P. (1990), private communication.  
 Brouillard, F. (1983), in *Atomic and Molecular Processes in Controlled Thermonuclear Fusion*, edited by C. J. Joachain and D. E. Post, Plenum, New York.  
 Cheung, C. C., Kim, Y. K. & Desclaux, J. P. (1979), *Electric Dipole Quadrupole and Magnetic Dipole Transition Probabilities of Ions Isoelectronic to the First Row Atoms, Li through F*, *At. Data and Nucl. Data Table* **24**, 111.  
 Cowan, R. D., Hobbs, L. M. & York, D. G. (1982), *Theoretical Oscillator Strengths for 21 Spin-Forbidden Lines of C, N, O, Al, and Si*, *Astrophys. J.* **257**, 373.  
 Dittner, P. F. (1988), *Phys. Scr.* **T22**, 65.  
 Doschek, G. A., (1985), *Diagnostics of Solar and Astrophysical Plasmas Dependent on Autoionization Phenomena*, in *AUTOIONIZATION*, ed. A. Temkin (New York: Plenum Publishing Corp.) p. 171.  
 Doschek, G. A., Feldman, U., Bhatia, A. K. & Mason, H. E. (1978), *Astrophys. J.* **226**, 1129.  
 Doschek, G. A., Feldman, U., VanHoosier, M. E., & Bartoe, J. -D. F. (1976), *Astrophys. J. Suppl. Ser.* **31**, 417.  
 Ellis, D. G. (1989), *Problems in the Calculation of Intercombination Line Strengths*, *Phys. Scr.* **40**, 12.  
 Ellis, D. G. & Martinson, I. (1984), *The  $3s3p^3$   $^5S^o$  Level in the Silicon Isoelectronic Sequence*, *Phys. Scr.* **30**, 225.  
 Foukal, P. and Hinata, S. (1991), *Solar Physics* **132**, 307.  
 Gardner, L. D., Kohl, J. L., Lafyatis, G. P., Young, A. R., and Chutjian, A. (1986) *Rev. Sci. Instrum.* **57**, 2254.  
 Gau, J. N., and Henry, R. J. W. (1977), *Phys. Rev. A* **16**, 986.  
 Glass, R. & Hibbert, A. (1978), *The Use of the Breit Interaction: The  $^3P \rightarrow ^1S_0$  Intercombination in Beryllium-like Systems*, *J. Phys. B* **11**, 2413.  
 Griem, Hans R. (1964), *Plasma Spectroscopy*, McGraw-Hill Book Co., NY.  
 Griffin, D. C. (1989), (private communication).  
 Griffin, D. C. (1989), *Phys. Scr.* **T28**, 17.  
 Griffin, D. C., Pindzola, M. S., and Bottcher, C. (1985), *Phys. Rev. A* **33**, 3124.  
 Harmin, D. A. (1987), *Phys. Rev. Lett.* **57**, 1570.  
 Huang, K.-N. (1985), *Energy-level scheme and transition probabilities of Si-like ions*, *At.*

- Data Nucl. Data Tables **32**, 503.
- LaGattuta, K. J. (1985), J. Phys. B **18**, L467.
- LaGattuta, K. J., Nasser, I., and Hahn, Y. (1985), Phys. Rev. A **33**, 2782.
- Lafyatis, G. P., Kohl, J. L., Gardner, L. D., (1987), Rev. Sci. Instrum. **58**, 383.
- Laughlin, C., Constantinides, E. R. & Victor, G. A. (1978), *Two-Valence-Electron Model-Potential Studies of the Be I Isoelectronic Sequence*, J. Phys. B **11**, 2243.
- Leo, William R. (1987), *Techniques for Nuclear and Particle Physics Experiments*, p. 90 (Springer-Verlag: Berlin).
- Mann, J. B. (1980), quoted in Merts, A. L., Mann, J. B., Robb, W. D., and Magee Jr., N. H., *Electron Impact Excitation of Positive Ions: A Collection of Positive Data*, Los Alamos informal report LA-8267-MS, 1980.
- Mavrogenes, G. S., Rambler, W. J., and Turner, C. B. (1965), *A Source for Multiply-Charged Ions*, IEEE Trans. Nucl. Sci. NS-12, 769.
- McLaughlin, D. J. and Hahn, Y. (1983), Phys. Rev. A **27**, 1389.
- Moos, H. W., Durrance, S. T., Skinner, T. E., Feldman, P. D., Bertaux, J. L. & Festov, M. C. (1983), *IUE Spectrum of the Io Torus: Identification of the  $^5S_2 \rightarrow ^3P_{2,1}$  Transition of S III*, Astrophys. J. **275**, L19.
- Nussbaumer, H. & Storey, P. J. (1978), *The C III Transition Probabilities*, Astron. Astrophys. **64**, 139.
- Raymond, J. C. (1988), *Hot Thin Plasmas in Astrophysics*, Klumer Academic, 3.
- Raymond, J. C. & Dupree, A. K. (1978), Astrophys. J. **222**, 379.
- Reisenfeld, D. B., Raymond, J. C., and Young, A. R. (1992), Ap. J. Letters (in press).
- Reisenfeld, D. B. (1992), Ap. J. (in press).
- Robb, W. D. (1980) quoted in Merts, A. L., Mann, J. B., Robb, W. D., and Magee Jr., N. H., *Electron Impact Excitation of Positive Ions: A Collection of Positive Data*, Los Alamos informal report LA-8267-MS, 1980.
- Smith, P. L., Johnson, B. C., Kwong, H. S., Parkinson, W. H. & Knight, R. D. (1984a), Physica Scripta **T8**, 88.
- Smith, P. L., Magnusson, C. E. & Zetterberg, P. O. (1984b), *Laboratory Identification of the  $3s^2 3p^2 \ ^3P_{2,1} - 3s 3p^3 \ ^5S_2^o$  Intersystem Lines of S III*, Astrophys. J. (Lett.) **277**, L79.
- Young, A. R., Chutjian, A., Gardner, L. D., Kohl, J. L., Lafyatis, G. P., and Savin, D. W. (1992), *Measurement of  $C^{3+}$  Dielectronic Recombination in a Known External Field*, Phys. Rev. A, in press.
- Young, A. R. (1990) Ph.D. thesis, Harvard University.